



18th International Conference Metal Forming 2020

Simulative basic investigation for a new forming process punch-hole-rolling

Maximilian Knoll^{a,*}, Fabian Mühl^b, Peter Groche^a, Volker Schulze^b

^aTechnical University of Darmstadt, Institute for Production Engineering and Forming Machines, 64287 Darmstadt, Germany

^bKarlsruhe Institute of Technology, Institute of Applied Materials (IAM-WK), 76131 Karlsruhe, Germany

* Corresponding author. Tel.: +49-6151-16-23148 ; fax: +49-6151-16-23142. E-mail address: knoll@ptu.tu-darmstadt.de

Abstract

Future products will require new forming processes in order to meet the increasing requirements for innovative products. These processes will enable new possibilities in product manufacturing and the control of product properties beyond geometry control. For this purpose, a new process called punch-hole-rolling has been developed, which enables the production of a double-sided collar in thin sheet structures. Punch-hole-rolling is a two-stage process combination of conventional shear cutting and novel rolling which is carried out in one tool. The process combination allows to derive product data from the punching process for the control of the flexible hole-rolling in order to control product properties such as geometry, hardness and microstructure. In order to increase the process understanding and classification, an FE-simulation is built and validated by experiments.

© 2020 The Authors. Published by Elsevier B.V.

This is an open access article under the CC BY-NC-ND license (<http://creativecommons.org/licenses/by-nc-nd/4.0/>)

Peer-review under responsibility of the scientific committee of the 18th International Conference Metal Forming 2020

Keywords: property control; metal forming; punch-hole-rolling; process simulation

1. Introduction

Current scientific and industrial research focus on increasing the degree of automation of production processes [12]. This form of automation focuses on the control of product properties instead of controlled process or machine variables [4]. This is to ensure that disturbance variables in manufacturing processes do not lead to unacceptably large deviations of product properties.

In addition to striving for a higher degree of automation, the desire for a more efficient use of resources also requires new concepts for the control of forming processes, since productive forming processes for metals such as steel or aluminum alloys are often used in the manufacture of highly loaded components [5]. As the strength of the materials increases, their lightweight construction quality increases, but at the same time the permissible process windows shrink. Consequently, the process fluctuation increases [3, 15]. The challenge in designing future forming processes is therefore to ensure high product quality even under fluctuating process conditions. Allwood et al. [1] have shown that this challenge can be met by means of closed-loop controlled forming processes. While the control of the geometrical properties of workpieces and products has already been successfully implemented in several studies for conventional forming processes, the control

of other product properties, such as material conditions, has hardly been successfully implemented so far. The main obstacle for the control of material properties, which has not been carried out so far, are the gaps in knowledge about inline sensor technology for describing material states which must be integrated into the forming process. Furthermore, there is a lack of qualified observers making it possible to draw conclusions about the workpiece or product properties of interest from measurable variables. In addition, flexible processes and machines with sufficient degrees of freedom are needed to allow the control of geometry and material properties [11]. However, requirements for bearing seats go beyond the geometric properties achieved so far. Requirements for bearing housings, such as hardness, surface quality, stiffness and material structure cannot be influenced by conventional forming processes like collar forming and flow drilling. For this reason, bearing housings have so far been produced by metal cutting, which contradicts the idea of resource efficiency. Additionally, forming technology offers higher material utilization with higher material strength and optimal grain flow.

Therefore, the punch-hole-rolling process was developed to investigate suitable control approaches for the description of material properties. The degrees of freedom of the process allow the control of geometry, hardness, material structure and

surface quality. In order to be able to derive first observers for the control of material properties, the process must first be fundamentally understood. For this purpose, first correlations between process control variables, the final geometry and the process force are investigated experimentally and simulatively.

Nomenclature

c	calibration factor
d	diameter
E	work
F	force
k_{tool}	tool stiffness
m	mass
r	radius
\dot{r}	radial feed rate
R	specific heat capacity
s_0	sheet thickness
t	time
T	temperature
u	displacement
u'	angle
α	heat transfer coefficient
ω	rotational speed

2. Process Description

Punch-hole-rolling is a combination of shear cutting and a rolling process. During the process, a single tool is used to perform shear cutting and rolling. Apart from the punch-roll die, no other driven tools are required. Figure 1 shows the process stages of punch-hole-rolling. At the beginning of the process a conventional punching process according to DIN 8588 is carried out, see Fig. 1 a). This produces a shearing surface with draw-in, breakage and burr zone typical of punching. For the subsequent rolling process, the punching die is first removed from the contact area of the cutting punches, see Fig. 1 b). For example, this can be achieved by design using springs. In the subsequent rolling process, see Fig. 1 c), the punch is moved along a free path. The continuous feed of the tool in radial direction results in an elastic-plastic deformation of the punching surface. In order to realize a rolling movement between tool and workpiece, the tool is rotatably mounted. Due to the plastic deformation, the cutting surface levels out at the beginning. The further tool feeding then splits the material into two collars similar to flow splitting [10, 16].

In contrast to flow splitting process, no additional support rolls are required for the sheet metal and the process takes place in the middle of the sheet instead of at the sheet's edges.

Punch-hole-rolling allows not only the production of rotationally symmetrical geometries but also non-rotationally symmetrical, conical, concave and convex contours. Furthermore, more complex geometries, such as cam plates, are conceivable due to an upstream nipple process.

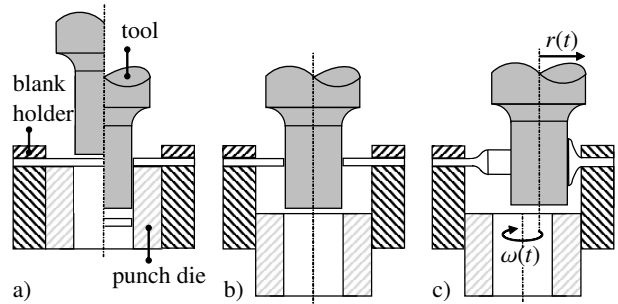


Fig. 1. Process steps of punch-hole-rolling.

3. Simulation

In order to improve the understanding of punch-hole-rolling process on a macroscopic level and to derive observer models for the control of geometry and material properties, a finite element simulation in *MarcMentat 2019* will be established. In the simulation, shear cutting and the resulting influences, such as cutting edge geometry and material changes, are neglected. The forming part is modelled as a rotationally symmetric cylinder with an inner diameter d_i and an outer diameter $d_o = 25$ mm, see Fig. 2. Boundary conditions are fixed the outer diameter in all six degrees of freedom u_i and u'_i .

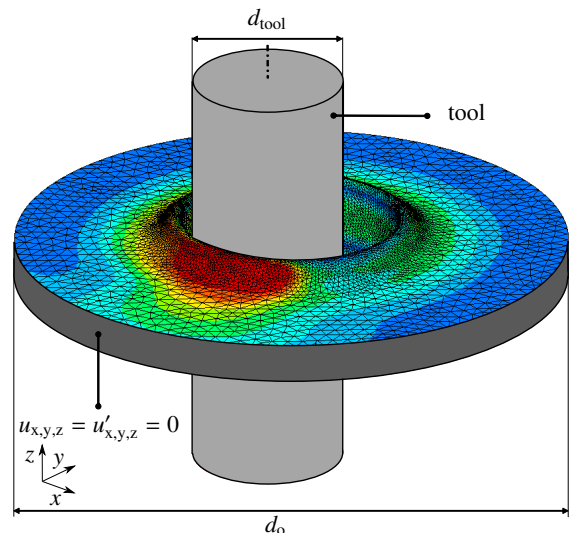


Fig. 2. Modeling of the simulation.

The forming tool is modeled as a rigid cylindrical body and driven by a freely programmable table in x, y direction. In the simulations, a spiral movement with constant feed rate in radial direction $\dot{r}(t)$ and rotational speed $\omega(t)$ is defined as the movement path. At the end of the process, a cylindrical motion path follows. Due to the tool movement present in the real process, the contact between tool and workpiece is assumed to be frictionless so that a rotation of the tool around the tool axis can be neglected.

Due to the high plastic deformation, a remesh algorithm is required to adjust the mesh quality during the simulation. Therefore, tetrahedron elements with four nodes used in combination with a robust Petran Tetra remesh algorithm. Initially, the whole workpiece is meshed with an element edge length of 0.8 mm. Remeshing is executed if there is penetration between tool and elements or if elements are stretched by more than 20%. Furthermore, a refinement depending on the node displacement is defined. For total node displacements more than 0.4 mm, an element edge length of 0.2 mm is remeshed. In the range from 0 mm to 0.4 mm of total node displacement, the element edge length is in the range between 0.8 mm and 0.2 mm.

An elastic-plastic isotropic approach is used as material model. The material parameters of DC04 (1.0338) are taken from the material database of *Simufact 2018*. By the equation of state

$$E_{\text{process}} = m \cdot R \cdot \Delta T \quad (1)$$

and the law of conservation of energy, the system energy can be calculated.

$$E_{\text{process}} = E_{\text{adiabat}} - E_{\text{air}} \quad (2)$$

Under the assumption of a constantly discharged heat flux,

$$E_{\text{air}} = \alpha \cdot A \cdot \Delta T \cdot \Delta t \quad (3)$$

the homogeneous temperature can be calculated.

$$\Delta T = \frac{E_{\text{adiabat}}}{m \cdot R + \alpha \cdot A \cdot \Delta t} \quad (4)$$

With a simulation time $\Delta t = 70$ s and a reshape from $d_0 = 4$ mm to $d_1 = 19$ mm with a thickness of $s_0 = 2$ mm, a total work of $\Delta E_{\text{adiabat}} = 500$ J results. Further parameters are given by $\alpha = 4,9 \text{ Wm}^{-2}\text{K}^{-1}$ and $R = 0,477 \text{ kJkg}^{-2}\text{K}^{-1}$. This leads to a temperature difference of $\Delta T = 77$ K. The real temperature, however, is below the calculated temperature due to the heat dissipated by convection. Thus, the temperature influence on the material data can be neglected in the simulation. The simulation is calculated implicitly with an "Adaptive Multi-Criteria" algorithm and a maximum step size of 0.002 s.

4. Experimental Setup

For experimental investigations of punch-hole-rolling, first tests are carried out on a conventional lathe (*Wagner Maschinen*, DSC200X900). In this case, the forming tool is placed on the tool slide, which realizes the radial feed rate as shown in Fig. 11. The rolling tool is a pivoted mounted shaft, which has an outer diameter of 8 mm. Two piezoelectric force sensors (*Kistler 9031A*), which measure the radial process forces, are placed between the bearing part and the lathe tool holder.

The force sensors are thereby preloaded to 50% of the maximum force so that they can measure tensile and compression forces. The preload of the sensors generates a secondary force flow, which flows through the preload screws.

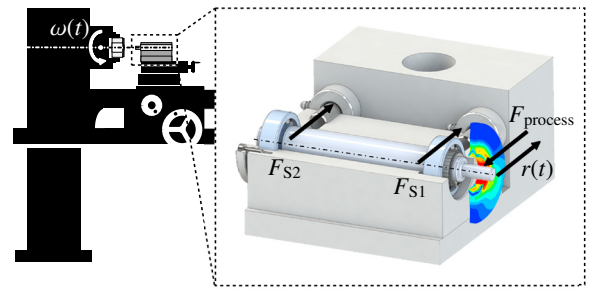


Fig. 3. Experimental process setup on a conventional lathe.

The preloaded measuring system is therefore calibrated on the *Zwick Roell 100*, whereby a combined calibration value for the measuring system is determined. With the calibration factor $c = 1.157$ and equation 5 the process force F_{process} can be determined.

$$F_{\text{process}} = c \cdot (F_{S1} + F_{S2}) \quad (5)$$

The sensor signals are amplified by a *Kistler 5067* amplifier to a voltage of ± 10 V. The tool is also equipped with a displacement sensor *Burster 8111* 150 mm, which measures the displacement in radial direction. All analog signals are collected, processed and recorded in a *National Instruments CompactRIO 9082* with a sampling rate of 500 Hz.

During the tests, the required hole is made on lathe by using an 8.1 mm HSS drill. Then the rolling tool (see Fig. 3) is positioned in the drilled hole. All degrees of freedom required for punch-hole-rolling are given by the lathe spindle and the cross slide. The spindle provides the rotary speed $\omega(t)$ and the cross slide the radial feed rate $\dot{r}(t)$. A constant rotation speed and feed rate is set up during the forming process. The start and end of the process is not programmable on the conventional lathe, so the operator initiates this.

5. Simulation Validation

At the beginning of the investigations, the simulation is validated by experiments. The validation of the simulation takes place on the basis of geometrical and physical parameters. The simulation is validated using material DC04 (1.0338). For this purpose, the following process parameters are used in simulation and experiment. Due to manufacturing deviations of the tool, a larger initial diameter is selected in the experiment than that produced during punching.

The simulation of geometric effects can be validated on the basis of the collar height. In contrast to the simulation, the collar height is determined outside the tool. A conventional caliper gauge is used as measuring device. The collar height of the simulation, however, is determined during the tool contact. In the experiments, non-symmetrical collars occur due to imperfections of the material and the bending of the tool. The collar height at the beginning of the process corresponds to the sheet thickness s_0 .

Table 1. Experiment and simulation parameters for validation.

	Test Set 1	Test Set 2
Material	DC04 (1.0338)	DC04 (1.0338)
Sheet thickness s_0	2 mm	2 mm
Tool diameter d_{tool}	8.0 mm	8.0 mm
Inner diameter d_i	8.1 mm	10.0 mm
Rotation speed ω	50 rpm	5 rpm
Feed rate \dot{r}	0.083 mm/s	0.083 mm/s

It can be seen in Fig. 4 that the collar height of the DC04 (1.0338) with different initial diameters d_i at the beginning of the simulation shows a good agreement with the experiments. The deviation between simulation and experiment increases with increasing inner diameter. This is why the collar height is larger in the simulation than in the experiment. It should be noted that friction is neglected in the simulation. Taking into account the friction in axial direction, the flow movement would be reduced and a lower collar height would be achieved. Furthermore, it can be seen that, the collar height approaches with increasing inner radius. This effect is much more significant in experiments. Due to the one-sided tool contact, the collar can be freely shaped during the process, which can result in collars of the same height under different process conditions.

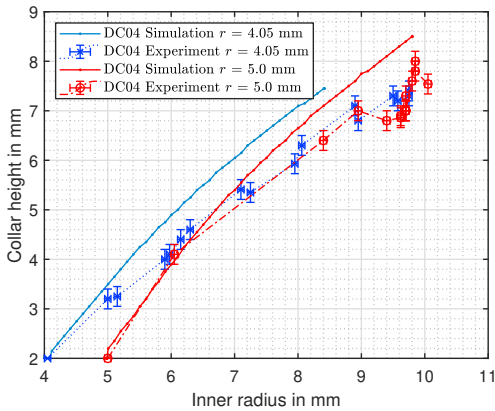
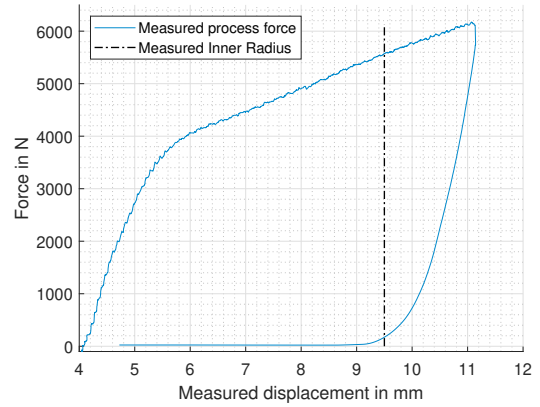


Fig. 4. Comparison of the simulated and experimental collar height.

Furthermore, the process forces will be compared with the simulation forces. Fig. 5 shows the experimental process force over the measured path. Due to the small tool stiffness, the measured inner radius of the sample differs from the measured path by approximately 1.5 mm.

Following [14] a linear stiffness in radial direction can be assumed for lathes. In order to determine the real process path, the tool stiffness k_{tool} is calculated from the measured force-displacement curve. Assuming a linear elastic system, a linearization is performed using the force-displacement curve (Fig. 5). From the linear approach

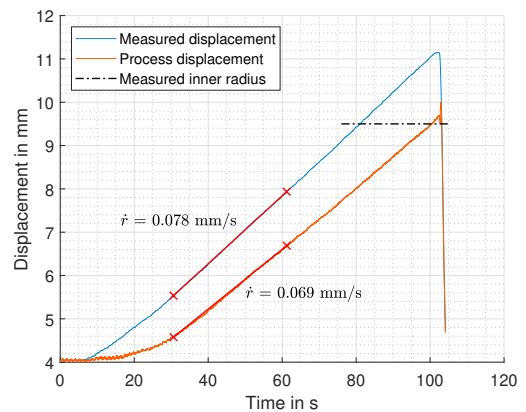
$$u_{\text{process}} = u_{\text{measured}} - k_{\text{tool}} \cdot F_{\text{process}} \quad (6)$$

Fig. 5. Experimental force-displacement diagram for $d_i = 8.1$ mm.

follows that at the point of maximum force the process radius corresponds to the measured inner radius r_{measured} . This allows to calculate the tool stiffness as shown in equation 7.

$$k_{\text{tool}} = \frac{u_{\text{measured}}(F_{\text{max}}) - r_{\text{measured}}}{F_{\text{max}}} \quad (7)$$

The resulting process path compared to the measured path is shown in Fig. 6. It can be seen that by taking into account the tool stiffness the resulting inner radius in the process path is achieved. In addition, Fig. 6 shows that process and measured feed rate deviate from the specified feed rate. The deviation of the measured feed rate results from the machine stiffness that exists between the measuring position and the spindle feed. Due to the tool stiffness, the feed rate acting in the process is reduced to 0.069 mm/s.

Fig. 6. Displacement before and after consideration of the tool stiffness by $d_i = 8.1$ mm.

The resulting force displacement and the simulation force are shown in Fig. 7. Initially, the forming force of the simulation is higher than the forming force of the experiments. The initial

deviation can be explained by an infinitely high tool stiffness in the simulation and the smoothing of surface in the experiment.

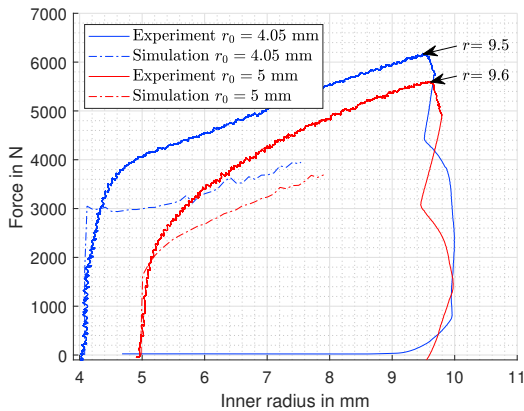


Fig. 7. Comparison of the force-displacement curves of experiment and simulation with $d_1 = 8.1$ mm.

As shown, the simulation force after the initial phase is below the experimentally determined process force. A constant offset remains between experiment and simulation. By increasing the experimental feed rate to 0.083 mm/s, the experimental process force would increase further, since a larger volume per time would be transformed.

Therefore, it can be assumed that the flow curves used in the simulation do not correspond to the experimental material data. For this reason, only quantitative and no qualitative statements can be made regarding stress effects in the workpiece.

6. Results

As already shown in Fig. 7 ($r_0 = 4.05$ mm), the process force increases to a local maximum at the beginning of the process. The local maximum results from the high radial initial contact, which is achieved with the same initial diameter and tool diameter. With increasing expansion, the radial contact area and forming force then decreases until the ratio of radial contact to increasing collar height is reversed. As a result, the contact area grows and with it the forming force, with a simultaneous increase in strain hardening until the end of the process. Therefore, the process limits depend on the geometric shape of tool on one hand and on the material properties of the workpiece on other hand.

The results obtained from the simulations can be used to improve the current understanding of the hole-rolling process. The description of the effective stress state is the most important aspect. This provides information for process classification and also allows conclusions to be drawn about the residual stresses acting in the component.

If the stress state acting on the tool is observed in a radial section through the workpiece while the tool is in contact with the workpiece, conclusions can be drawn for process classification. Fig. 8 shows the acting stresses in the radial and

tangential directions for different process steps of $r_1 = 4.7$ mm and $r_1 = 6.6$ mm. It can be seen that the process in the area of tool contact in both radial and tangential directions mainly has compressive stresses. As expected, the greatest compressive stresses are found in the middle of the sheet.

With increasing process progress, the tensile stresses in the edge area of the collar increase (Fig. 9 grey). The tangential tensile stresses in the upper collar area reach up to the tool contact.

Fig. 9 shows the unrolled surface of the formed inner diameter. The tool is in contact at 180° , as shown by the tangential compressive stresses. Outside the tool contact, however, mainly tangential tensile stresses occur. The greatest tensile stresses occur in the opposite rolling direction. In comparison to Fig. 8, compressive stresses act outside the tool contact area in the edge area of the double-sided collar.

This is accompanied by the expectation that material failure will occur in the contact area of the tool, in the upper and lower edge area of the collar. A material failure outside of the tool contact appears unlikely in the edge area of the collar due to the acting compressive stresses.

7. Process Classification

Forming processes can be classified on the basis of the stress conditions acting during the process. Forming processes are classified into tensile, compression, tension-compression, bending and shear stresses [6]. Rolling is one of the pressure forming processes. Rolling can also be classified on the basis of kinematics, tool geometry and workpiece geometry and into the groups of longitudinal rolling, transverse rolling and cross rolling [7]. Longitudinal rolling is defined as a process in which the rolled material is moved through the roll gap perpendicularly to the rolling axis. In cross rolling, the stock is rotated about its own workpiece axis without movement in the axial direction. Cross rolling is described as a process in which the rolling axes cross each other resulting in longitudinal feed.

For the production of functional surfaces in thin-walled structures, manufacturing technology already has methods such as collar forming, upset bulging and friction drilling available. Collar forming [8], which according to [6] belongs to the compression-tension forming processes, allows to produce one-sided collars. The perforated semi-finished product is formed into a collar using a punch and forming die. The collar thickness and surface roughness of the collar depends on the properties of the semi-finished product.

Upset bulging [9], belongs also to the tension-compression forming processes. In this process, pipes that are usually rotationally symmetrical are buckled by applying axial forces. By using upset bulging as a joining method in sheet metal structures, form-fitting, double-sided collars can be produced [2].

Another process for the production of functional surfaces in thin-walled structures is friction drilling. Friction drilling is a non-cutting drilling process which reduces the flow stress

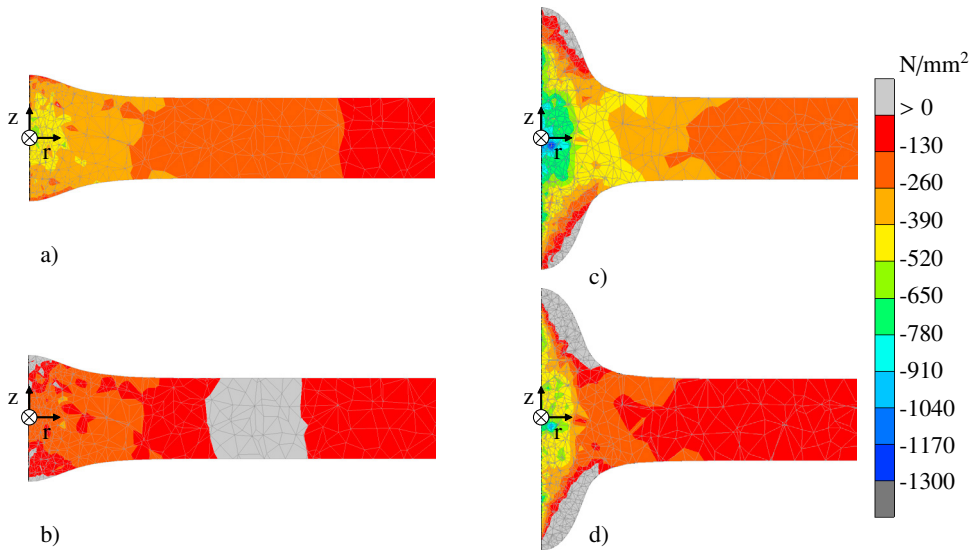


Fig. 8. Effective stress state during tool contact. a) Radial stress at $r_1 = 4.7$ mm; b) Tangential stress at $r_1 = 4.7$ mm; c) Radial stress at $r_1 = 6.6$; d) Tangential stress at $r_1 = 6.6$ mm.

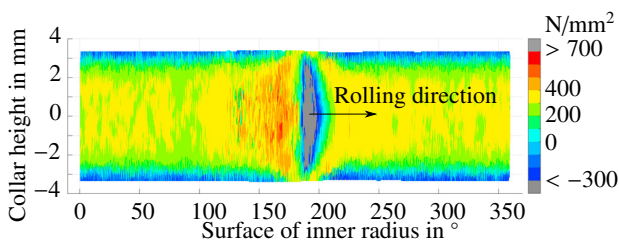


Fig. 9. Tangential stress on the surface of the inner radius at $r = 7.49$ mm.

limit due to the friction and temperature generated between tool and workpiece. The material is displaced by the drilling displacement, resulting in a non-symmetrical collar on both sides. [13]

Punch-hole-rolling is a combination of conventional shear cutting and a rolling process, whereby the feed motion can be realized by both the tool and the workpiece. Due to the compressive stresses resulting from punch-hole-rolling, the process can be assigned to the pressure forming processes. Comparing the process with the presented processes for the production of functional surfaces in thin-walled structures, punch-hole-rolling shows differences in the resulting collar in addition to the effective stresses. In comparison to collar forming and friction drilling, punch-hole-rolling allows symmetrical double-sided collars to be produced. The production of double-sided rotationally symmetrical collars is also possible with buckling. In comparison to the form-fitting collar of the upset bulging, the manufactured collar of the punch-hole rolling process is material-fitting.

8. Conclusion

On the basis of the experimental and simulative investigations, it has been shown that the punch-hole-rolling process is possible. However, the previous simulations showed discrepancies with regard to the collar height and the resulting process force, which is why the results only provide quantitative information about the process. It has to be taken into account that the simulations are based on material data from a material database and were not explicitly determined using the test material. In addition, the results showed that the process limits can be described by tangential tensile stresses in the collar edge area. Furthermore, the process could be classified as compression forming process, more precisely as rolling process, due to the effective stress conditions. Based on the experimental data obtained, first models for the analytical description of the geometric and material properties can be derived. An improvement of the simulations is needed for the analytical description of the process. Also an adapted material model is needed to increase the simulation quality. Furthermore, the influence of friction in the axial direction of the tool has to be investigated. In addition, a reduction of the simulation model has to be investigated in order to reduce the required computing effort. Additionally to the presented validations, a final validation of the acting residual stresses would be useful.

9. Acknowledgement

The authors would like to thank the German Research Foundation DFG for the support of the depicted research within the priority program ‘SPP2183’ through project no. ‘GR 1818/72–1’.

References

- [1] Allwood, J., Duncan, S., Cao, J., Groche, P., Hirt, G., Kinsey, B., Kuboki, T., Liewald, M., Sterzing, A., Tekkaya, A., 2016. Closed-loop control of product properties in metal forming. *CIRP Annals* 65, 573–596.
- [2] Almohallami, A., Rusch, M., Vucetic, M., Bouguecha, A., Bambach, M., Behrens, B.A., 2016. Joining by upset bulging at elevated temperatures. *Advanced Materials Research* 1140, 115–122.
- [3] Barthau, M., Liewald, M., 2017. New approach on controlling strain distribution manufactured in sheet metal components during deep drawing process. *Procedia engineering* 207, 66–71.
- [4] Behrens, B.A., Groche, P., Krüger, J., Wulfsberg, J.P., 2018. WGP-Standpunkt Industriearbeitsplatz 2025. Standpunkt-papier. Wissenschaftliche Gesellschaft für Produktionstechnik WGP e.V. Garbsen.
- [5] Breuer, D., Klocke, F., 2007. Bestimmung des Formänderungsvermögens bei der Kaltmassivumformung. Lehrstuhl für Technologie der Fertigungsverfahren.
- [6] DIN 8580, German Institute for Standardization, 2003. Manufacturing processes - terms and definitions, division. Beuth .
- [7] DIN 8583-2, German Institute for Standardization, 2003. Manufacturing processes forming under compressive conditions - part 2: Rolling; classification, subdivision, terms and definitions. Beuth .
- [8] DIN 8584-5, German Institute for Standardization, 2003. Manufacturing processes forming under combination of tensile and compressive conditions - part 5: Forming by raising; classification, subdivision, terms and definitions. Beuth .
- [9] DIN 8584-6, German Institute for Standardization, 2003. Manufacturing processes forming under combination of tensile and compressive conditions - part 6: Upset bulging; classification, subdivision, terms and definitions. Beuth .
- [10] Groche, P., Ringler, J., Shreehah, T.A., 2009. Bending–rolling combinations for strips with optimized cross-section geometries. *CIRP annals* 58, 263–266.
- [11] Groche, P., Scheitza, M., Kraft, M., Schmitt, S., 2010. Increased total flexibility by 3d servo presses. *CIRP annals* 59, 267–270.
- [12] Manyika, J., 2017. A future that works: Ai, automation, employment, and productivity. McKinsey Global Institute Research, Tech. Rep 60.
- [13] Miller, S.F., Tao, J., Shih, A.J., 2006. Friction drilling of cast metals. *International Journal of Machine Tools and Manufacture* 46, 1526 – 1535.
- [14] Nickols, F., Martin, K., 1992. “right diameter-first cut” lathe datuming probe , 291–301.
- [15] Polyblank, J.A., Allwood, J.M., Duncan, S.R., 2014. Closed-loop control of product properties in metal forming: A review and prospectus. *Journal of Materials Processing Technology* 214, 2333–2348.
- [16] Taplick, C., Rullmann, F., Groche, P., 2010. Further processing of ultrafine-grain materials. *International Journal of Material Forming* 3, 833–836.